

Quantum Speed Limit in Terms of Coherence Variations

Zi-yi Mai¹ and Chang-shui Yu^{1,*}

¹*School of Physics, Dalian University of Technology, Dalian 116024, P.R. China*

(Dated: October 14, 2024)

Coherence is the most fundamental quantum resource in quantum information processing. How fast a physical system gets coherence or decoherence is a critical ingredient. We present an attainable quantum speed limit based on the variation of quantum coherence subject to a dynamical process. It indicates that for a 2-dimensional quantum state, one can always find corresponding dynamics driving it to evolve along the geodesic to another state with certain coherence variation. As applications, we study the coherence quantum speed limits of the dephasing and dissipative dynamics. It is shown that the dephasing dynamics can saturate our coherence quantum speed limit, and the decoherence of the state with identical populations will be faster than others. However, the dissipative dynamics have the opposite behavior. In addition, we illustrate a stronger tightness of our bound for the mentioned dynamics by comparison.

I. INTRODUCTION

Quantum resources, including quantum coherence, entanglement, nonlocality, etc., play an essential role in quantum information processing tasks (QIPTs). In this sense, QIPTs can be understood as generating and consuming quantum resources. However, QIPTs imply that the generation of consumption of quantum resources should be as quick as possible to save QIPT time and avoid detrimental disturbance or decoherence, and so on. How fast can the resources be changed? Quantum speed limit (QSL) can answer this question by considering the least evolution time between two states with a certain amount of resources.

QSL was originally raised to describe the least time for the evolution between two states. The most typical QSL is the Mandelstam-Tam (MT) bound [1]

$$\tau \geq \tau_{\text{MT}}^{\perp} = \frac{\pi}{2\Delta E}, \quad (1)$$

A time-independent Hamiltonian provides a lower bound of the needed time to drive an arbitrary pure state to its orthogonal state. In other words, for the fixed energy variance, MT bound is the minimum evolution time by optimizing over all the potential state pairs and the Hamiltonian. Later, Margolus and Levitin introduced a new bound (ML bound) as [2]

$$\tau \geq \tau_{\text{ML}}^{\perp} = \frac{\pi}{2E}, \quad (2)$$

where E is the expected value of the system energy. Both the MT and ML bounds are attainable for the initial state with equal weight superposition of two eigenstates of the Hamiltonian [2, 3].

Up to now, QSL has attracted increasing interest and has been generalized in different scenarios [4, 5] including the QSLs for the mixed states [6, 7], time-dependent

Hamiltonian [8, 9], the geometric understandings [10–12] and so on [13]. In particular, the QSL has been generalized to the open systems [14–24]. It is shown that the lower bound of evolution time τ for a initial state ρ_0 and target state ρ_{τ} can be given as $\tau \geq d(\rho_0, \rho_{\tau}) / \langle d(\rho_t, \rho_{t+dt}) / dt \rangle_{\tau}$, where d is the distance of the two states and $\langle d(\rho_t, \rho_{t+dt}) / dt \rangle_{\tau} = \frac{1}{\tau} \int_0^{\tau} d(\rho_t, \rho_{t+dt})$ is the time-average evolution speed [25]. For example, Refs. [26, 27] developed the geometrical QSL based on the Bures angle and explained the evolution speed as the quantum Fisher information. Ref. [28] presented the QSL bound based on the trace distance and studied the environmental effect on the saturation of the QSL bound. The non-Markovian effect [27, 29–32], the effect of the Hamiltonian of an open quantum system [28, 33–36] and the role of coherence [37–39] are also addressed for the QSL. QSL has even been extended to the classical systems [40, 41]. QSLs are also widely studied in various quantum processes such as optimal control [42], quantum metrology [43–45], quantum battery [46, 47], precision thermometry [48], state preparation [49] and so on [50–53]. Recently, Ref. [54] considered the QSL of resource variation rather than the evolution between state pairs. Later, many studies were carried out for speed limit bound of the resource variation, including coherence [55, 56] and entanglement [57–60].

Quantum coherence is the most typical feature of quantum mechanics, distinguishing it from the classical world. It is also a crucial resource in many applications [61–80]. How fast does a physical system get coherent or decoherent? In some cases, this question potentially reveals the minimum time for the transition between quantum and classical features of a system. Although Ref. [39] provided a lower bound on the time required for coherence changes with von Neumann entropy as a coherence measure, whether the lower bound is attainable remains open. We will revisit the question in terms of a different coherence measure, and we find that the fastest decoherence speed is attainable under the purely Markovian dephasing channel.

This paper presents a QSL of the coherence variation regarding the skew information as the coherence measure

* ycs@dlut.edu.cn

[81]. Our bound is attainable for any 2-dimensional state undergoing proper dephasing dynamics. As applications, we study the coherence of QSLs for the dephasing and dissipative dynamics. We find that the dephasing dynamics can induce faster decoherence for the states with equal populations, and we further discuss the environmental effect on saturating our bound, but the dissipative dynamics have the opposite behavior. We also derive the conditions for the saturations of our QSL. This paper is organized as follows. We start with a brief introduction of the coherence measure. Then, we derive a quantum speed limit bound based on the coherence measure. Then, we apply the coherence QSLs to the dephasing and dissipative dynamics and the attainability and tightness of our QSL. Finally, we summarize the paper with some discussions.

II. COHERENCE SPEED LIMIT

To begin with, let's first introduce the coherence measure based on the skew information [81]. Under the framework of the quantification of the coherence [77], the coherence in terms of the skew information is defined as [81]

$$C(\rho) = \min_{\sigma \in \mathcal{I}} [1 - A^2(\rho, \sigma)] \quad (3)$$

subject to the given basis $\{|k\rangle\}_{k=1}^N$, where $A(\rho, \sigma) = \text{Tr} \sqrt{\rho \sqrt{\sigma}}$ is the quantum affinity [82, 83]. It is found that incoherent states can be written as $\sigma = \sum_{k=1}^N p_k |k\rangle \langle k|$. In particular, the coherence measure in Eq. (3) can be analytically calculated for any given finite dimension.

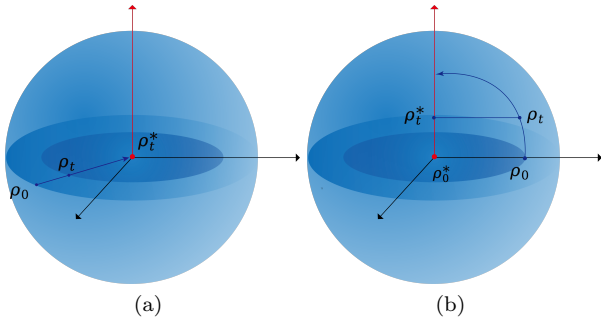


FIG. 1. The evolution trajectory in the Bloch representation. The dark blue arrow is the evolution trajectory, and the red arrow indicates the incoherent set. (a) the evolution trajectory coincides with a geodesics connecting ρ_0 and ρ_0^* , and $\rho_t^* = \rho_0^*$ is satisfied for $\forall t \in [0, \tau]$. (b) evolution trajectory under a non-optimal decoherence channel.

Based on the above-given coherence measure $C(\rho)$, we'd like to employ the metric of state distance as

$$\Theta(\rho, \sigma) = \arccos A(\rho, \sigma). \quad (4)$$

It is obvious that if σ in Eq. (4) is the closest incoherent state to ρ , namely, σ is the incoherent state maximizing

$\Theta(\rho, \sigma)$ in Eq. (4), one can easily relate the distance with the coherence measure $C(\rho)$ as

$$\begin{aligned} \min_{\sigma \in \mathcal{I}} \Theta(\rho, \sigma) &= \arccos \left\{ \max_{\delta \in \mathcal{I}} A(\rho, \sigma) \right\} \\ &= \arccos \sqrt{1 - \min_{\sigma \in \mathcal{I}} [1 - A^2(\rho, \sigma)]} \\ &= \arccos \sqrt{1 - C(\rho)}. \end{aligned} \quad (5)$$

$C(\rho)$ is the sine value of the minimum angle between ρ and the incoherent states subject to Eq. (4). Even though $\min_{\sigma \in \mathcal{I}} \Theta(\rho, \sigma)$ monotonically depends on the coherence $C(\rho)$, $\min_{\sigma \in \mathcal{I}} \Theta(\rho, \sigma)$ is an 'addressed' coherence instead of a strict coherence measure. For convenience, we use ρ^* to represent the closest incoherent state to ρ .

Next, we'd like to consider the dynamic evolution of ρ_t in the time interval $t \in [0, \tau]$. If $C(\rho_0) > C(\rho_\tau)$ one can obtain the following inequality:

$$\begin{aligned} &\arccos \sqrt{1 - C(\rho_0)} - \arccos \sqrt{1 - C(\rho_\tau)} \\ &= \Theta(\rho_0, \rho_0^*) - \Theta(\rho_\tau, \rho_\tau^*) \leq \Theta(\rho_0, \rho_\tau^*) - \Theta(\rho_\tau, \rho_\tau^*) \\ &\leq \Theta(\rho_0, \rho_\tau) \leq \int_0^\tau dt \Theta(\rho_t, \rho_{t+dt}), \end{aligned} \quad (6)$$

The final two inequalities are obtained using the triangle inequality for distance function Θ . Consider the infinitesimal time interval dt , one can get the distance between the initial state ρ_t and the final state ρ_{t+dt} as

$$\Theta^2(\rho_t, \rho_{t+dt}) = \text{Tr} \left(\frac{d}{dt} \sqrt{\rho_t} \right)^2, \quad (7)$$

which is the Wigner-Yanase metric and is also a quantum extension to the classical Fisher information [83], we present the derivation of the metric in Appendix C. Especially for the closed system, the Wigner-Yanase metric is reduced to the skew information [16, 25]. For the open system, one can obtain a similar understanding of the Wigner-Yanase metric to the closed system, as shown in Appendix A.

Similarly, for the case of $C(\rho_0) < C(\rho_\tau)$, we have

$$\begin{aligned} &\arccos \sqrt{1 - C(\rho_\tau)} - \arccos \sqrt{1 - C(\rho_0)} \\ &= \Theta(\rho_\tau, \rho_\tau^*) - \Theta(\rho_0, \rho_0^*) \leq \Theta(\rho_\tau, \rho_0^*) - \Theta(\rho_0, \rho_0^*) \\ &\leq \Theta(\rho_0, \rho_\tau) \leq \int_0^\tau dt \Theta(\rho_t, \rho_{t+dt}). \end{aligned} \quad (8)$$

Summarizing Eq. (6) and Eq. (8), one will directly arrive at the following theorem.

Theorem 1. -For a dynamical evolution from the state ρ_0 to ρ_τ , the time τ required for the coherence variation Δ_C is lower bounded by

$$\tau \geq \tau_{\text{CSL}} = \frac{|\Delta_C|}{\left\langle \sqrt{\text{Tr} \left(\frac{d}{dt} \sqrt{\rho_t} \right)^2} \right\rangle_\tau} = \frac{|\Delta_C|}{\left\langle \sqrt{\frac{1}{4} \mathcal{I}_F + 2 \mathcal{I}_{W-Y}} \right\rangle_\tau}, \quad (9)$$

where $\Delta_C = \arccos \sqrt{1 - C(\rho_\tau)} - \arccos \sqrt{1 - C(\rho_0)}$ and $\langle A \rangle_\tau = \frac{1}{\tau} \int_0^\tau dt A$ denotes the time average quantity. In particular, for the eigendecomposition $\rho_t = U_t \Lambda_t U_t^\dagger$ with $[\Lambda_t]_{ij} = \lambda_j \delta_{ij}$, $\mathcal{I}_F = 4 \sum_j \left(\frac{d}{dt} \sqrt{\lambda_j} \right)^2$ and $\mathcal{I}_{W-Y} = -\frac{1}{2} \text{Tr} [\sqrt{\rho_t}, H_t]^2$ are the classical Fisher information and the Wigner-Yanase skew information with $H_t = i\dot{U}_t U_t^\dagger$.

Proof. The inequality in Eq. (9) is the direct result of combining Eq. (6) and Eq. (8). The second equality holds based on Appendix A. \square

Eq. (9) is the main result of this paper. It gives the lower bound of required time for coherence variation for any dynamical process. The minimum time among all potential dynamical processes is the QSL subject to a given coherence variation. It is mainly shown that the coherence 'variation speed' is the collective contributions of the classical Fisher information and the skew information, which quantifies the sensitivity of the state ρ_t to a CPTP map due to classical and quantum effects, respectively [84]. In the next section, we will show that our bound is attainable, which means a dynamical process exists, converting a state to another state with the given coherence variation in the exact evolution time τ_{CSL} .

Our QSL of coherence shows an intuitive geometrical picture sketched in FIG. 1 in the Bloch representation. As is shown in FIG. 1 (a), we draw the shortest evolution trajectory from a given state ρ_0 towards another state ρ_t and even to an incoherent state. In this case, the speed limit inequality given in Eq. (9) is saturated, and the evolution trajectory coincides with the geodesics. In this evolution process, one can find that the optimal incoherent state for the coherence is always the same as the one for the initial state, i.e., for $\forall t \in [0, \tau]$, $\rho_t^* = \rho_0^*$. On the contrary, FIG. 1 (b) demonstrates the evolution trajectory deviating from the geodesics. This evolution trajectory is not optimal for decoherence; in this case, the speed limit bound is unsaturated.

III. APPLICATIONS AND THE ATTAINABILITY

Dephasing dynamics. To demonstrate the attainability, let's consider a concrete example as an application. Suppose that a two-level atom interacts with a bosonic reservoir, then the Hamiltonian governing the evolution of the total system is

$$H_{\text{tot}} = \frac{1}{2} \omega_0 \sigma_z + \sum_j \omega_j b_j^\dagger b_j + \sum_j g_j \sigma_z b_j^\dagger + \text{h.c.}, \quad (10)$$

where ω_0 is the atomic transition frequency, b_j is the annihilation operator of the j th mode in the bosonic reservoir, ω_j is the frequency of the j th mode harmonic oscillator, and g_j is the coupling strength of atom and the j th mode of the reservoir. In Schrödinger representation, one can obtain the master equation for the atomic system as

[85]

$$\dot{\rho}_t = -i[H_0, \rho] + \frac{\gamma_t}{2} (\sigma_z \rho_t \sigma_z - \rho_t), \quad (11)$$

where $H_0 = \frac{1}{2} \omega_0 \sigma_z$ is the free Hamiltonian, and γ_t denotes the dephasing rate. Note that γ_t can take different expressions in the different approximations, which can cover the non-Markovian and Markovian cases [85]. In the Markovian case, γ_t typically takes a positive constant. Let the initial state be

$$\rho_0 = \begin{pmatrix} 1 - \rho_{11} & \rho_{01} \\ \rho_{01}^* & \rho_{11} \end{pmatrix}, \quad (12)$$

one will immediately solve Eq. (11) and obtain the state ρ_t as

$$\rho_t = \begin{pmatrix} 1 - \rho_{11} & \rho_{01}(t) \\ \rho_{01}^*(t) & \rho_{11} \end{pmatrix}, \quad (13)$$

with $\rho_{01}(t) = \rho_{01} e^{-\int_0^t dt' \gamma_{t'} - i\omega_0 t}$.

To show the attainable QSL, we first consider the case $\rho_{11} = \frac{1}{2}$. In this case, one can calculate the square root of Eq. (13) and get

$$\sqrt{\rho_t} = \frac{1}{2} \begin{pmatrix} \sqrt{p_1} + \sqrt{p_2} & (\sqrt{p_1} - \sqrt{p_2}) e^{i\phi} \\ (\sqrt{p_1} - \sqrt{p_2}) e^{-i\phi} & \sqrt{p_1} + \sqrt{p_2} \end{pmatrix}, \quad (14)$$

where $p_1 = \frac{1}{2} + |\rho_{01}(t)|$ and $p_2 = 1 - p_1$ are the eigenvalues of the density matrix ρ_t , and $\phi = \text{Arg} \{ \rho_{01}(t) \}$. Thus, according to Theorem 1, one can calculate the metric as

$$\Theta^2(\rho_t, \rho_{t+dt}) = \text{Tr} \left(\frac{d}{dt} \sqrt{\rho_t} \right)^2 = \frac{1}{4} \mathcal{I}_F + 2\mathcal{I}_{W-Y}, \quad (15)$$

where the classical Fisher information \mathcal{I}_F and the Wigner-Yanase skew information \mathcal{I}_{W-Y} are given as

$$\mathcal{I}_F = 4 \sum_{j=0}^1 \left(\frac{d}{dt} \sqrt{p_j} \right)^2 = 4 \frac{|\rho_{01}(t)|^2}{1 - 4|\rho_{01}(t)|^2} \gamma_t^2 \quad (16)$$

and

$$\mathcal{I}_{W-Y} = -\frac{1}{2} \text{Tr} [\sqrt{\rho_t}, H_0]^2 = \frac{\omega_0^2}{2} \left(\frac{1}{2} - \sqrt{\frac{1}{4} - |\rho_{01}(t)|^2} \right), \quad (17)$$

respectively. It is obvious that the Wigner-Yanase skew information \mathcal{I}_{W-Y} given in Eq. (17) corresponds to the contribution of the free Hamiltonian H_0 . The classical Fisher information \mathcal{I}_F given in Eq. (16) denotes the contribution of the dephasing process.

Integrating the square root of Eq. (15) from 0 to τ ,

one can immediately find that

$$\begin{aligned}
& \int_0^\tau dt \sqrt{\frac{1}{4}\mathcal{I}_F + 2\mathcal{I}_{W-Y}} \geq \int_0^\tau dt \sqrt{\frac{1}{4}\mathcal{I}_F} \\
& \geq \left| \int_0^\tau dt \frac{|\rho_{01}(t)|}{\sqrt{1-4|\rho_{01}(t)|^2}} \gamma_t \right| = \left| \int_0^\tau dt \frac{\frac{d}{dt}|\rho_{01}(t)|}{\sqrt{1-4|\rho_{01}(t)|^2}} \right| \\
& = \left| \frac{1}{2} (\arcsin 2|\rho_{01}(\tau)| - \arcsin 2|\rho_{01}|) \right| \\
& = \left| \arcsin \sqrt{\frac{1}{2} - \sqrt{\frac{1}{4} - |\rho_{01}(\tau)|^2}} - \arcsin \sqrt{\frac{1}{2} - \sqrt{\frac{1}{4} - |\rho_{01}|^2}} \right| \\
& = \left| \arccos \sqrt{\frac{1}{2} - \sqrt{\frac{1}{4} - |\rho_{01}(\tau)|^2}} - \arccos \sqrt{\frac{1}{2} - \sqrt{\frac{1}{4} - |\rho_{01}|^2}} \right| \\
& = |\Delta_C|,
\end{aligned}$$

where we have used the equality $\arcsin \sqrt{\frac{1}{2} - \sqrt{\frac{1}{4} - x^2}} = \frac{1}{2} \arcsin 2x$. Besides, according to Ref. [81], we have $C(\rho) = 1 - \sum_k \langle k | \sqrt{\rho} | k \rangle^2 = 1 - \frac{1}{2} (\sqrt{p_1} + \sqrt{p_2})^2 = \frac{1}{2} - \sqrt{\frac{1}{4} - |\rho_{01}(t)|^2}$, which corresponds to the final result in Eq. (19). The first inequality saturates for the vanishing W-Y skew information, which can be achieved if the two energy levels are degenerate, i.e., $\omega_0 = 0$. Of course, one can also, at least in principle, consider a particular engineered noise $\xi(t)$ similar to Ref. [28] to eliminate the frequency ω_0 and mimic a purely dephasing dynamics.

The second inequality of Eq. (18) saturates if γ_t doesn't change its sign in the internal $t \in [0, \tau]$. Note that γ_t can take negative values within some time intervals due to the information exchange between the system and environment in a non-Markovian regime. Thus, Eq. (19) can safely saturate in the Markovian regime. However, some non-Markovian decoherence processes can also saturate Eq. (19). Let's consider the dephasing rate [85, 86]

$$\gamma_t = \int d\omega J(\omega) \coth\left(\frac{\omega}{2k_B T}\right) \frac{\sin \omega t}{\omega}, \quad (20)$$

where $J(\omega)$ denotes the Ohmic-like spectral density of the reservoir, and in the low-temperature limit, $J(\omega)$ can be given as

$$J(\omega) = \frac{\omega^k}{\omega_c^{k-1}} e^{-\frac{\omega}{\omega_c}} \quad (21)$$

with cutoff energy ω_c , and k describing the sub-Ohmic ($k < 1$), Ohmic ($k = 1$) and super-Ohmic ($k > 1$) environment. Under the zero temperature limit, the dephasing rate can be expressed as

$$\gamma_t = \omega_c (1 + \omega_c^2 t^2)^{-k/2} \Gamma(k) \sin[k \arctan(\omega_c t)] \quad (22)$$

with the Gamma function Γ . We provide the numerical result of τ_{CSL}/τ with different evolution times τ for the

super-Ohmic environment under the non-Markovian effect in FIG. 2, from which one can see that our bound saturates within the time interval ($\tau \leq 1$) with the positive dephasing rate but unsaturated when it turns to a negative value as increasing evolution time ($\tau > 1$). The above cases mainly belong to the decoherence. The coherence-generating process can also happen along the geodesics at some time intervals. In FIG. 2, one can find that the dephasing rate becomes negative from the moment $t^* = 1$, and our QSL bound is saturated. To sum up, one can find that the non-Markovian effect (with γ_t changing sign in $[0, \tau]$) and the free Hamiltonian H_0 can increase the length of the evolution trajectory and hence make the dynamics deviate the geodesics.

The above calculation indicates that the 2×2 density matrix with identical diagonal entries is the optimal state to be accelerated to the maximum decoherence speed. ρ_t approaches the incoherent state set along the geodesics under purely dephasing dynamics with the Markovian regime and the vanishing free Hamiltonian, meanwhile the geodesics connecting ρ_0 and ρ_τ travels through ρ_0^* , i.e., $\rho_t^* = \rho_0^*, \forall t \in [0, \tau]$.

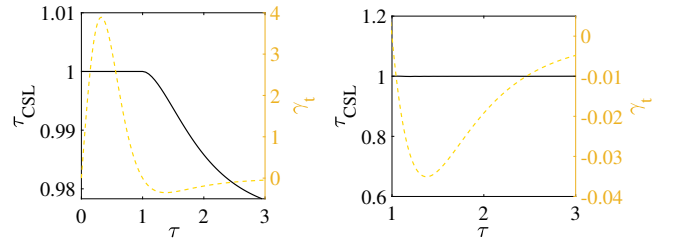


FIG. 2. (Left) The ratio τ_{CSL}/τ and dephasing rate γ_t vs evolution time τ . (Right) The ratio τ_{CSL}/τ and dephasing rate γ_t vs evolution time τ , and let the initial instant locates at $t^* = 1$. Both are considered in the non-Markovian process ($k = 4$).

We want to emphasize that for any 2×2 density matrix, there always exists an equal-population representation, where the diagonal entries of the density matrix are the same, i.e., $\rho_{11} = \frac{1}{2}$ in Eq. (12). Such a representation can be easily realized by applying the unitary transformation $U = \frac{1}{\sqrt{2}} \begin{pmatrix} 1 & ie^{i\phi} \\ 1 & -ie^{i\phi} \end{pmatrix}$. We can impose the above dephasing process under the Markovian regime in this representation and obtain similar results. In this sense, one can conclude that for any initial state, we can always find proper dephasing dynamics such that the system's coherence is degraded along the geodesics of the state evolution. Namely, our coherence QSL is attainable.

We also numerically study the dephasing dynamics with different initial states. We set $\rho_{11} = \sin^2 \frac{\theta}{2}$ and $\rho_{01} = \sin \frac{\theta}{2} \cos \frac{\theta}{2}$. The decay rate is selected as $\gamma_t = 2$, and the frequency difference is zero $\omega_0 = 0$. FIG. 3 (Left) shows the result, and meanwhile, we also attach the numerical result presented in Ref. [39] for comparison. It can be seen that our speed limit bound shows prefer-

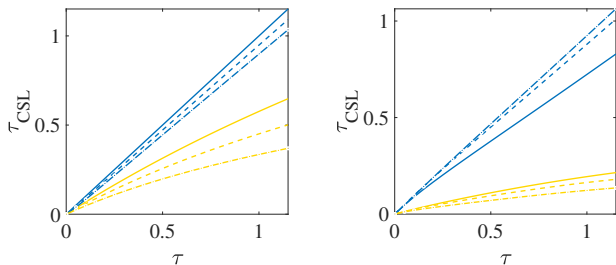


FIG. 3. The actual evolution time τ under the purely dephasing channel (Left) and the amplitude damping channel (Right) vs the speed limit time τ_{CSL} . The blue lines and the yellow lines are obtained by our coherence QSL time τ_{CSL} and that in Ref. [39], respectively, and the solid, dash and dash-dot lines represent the parameters $\theta = \frac{\pi}{2}$, $\frac{\pi}{3}$ and $\frac{\pi}{4}$ of the initial state, respectively.

able tightness for this model. The dephasing dynamics subject to the states with non-identical diagonal entries show a relatively slow decoherence speed. Namely, they always lead to $\tau > \tau_{\text{CSL}}$, which means these evolution trajectories deviate the geodesics, and the optimal decoherence dynamics allow the initial state evolves along the geodesics towards its closest coherent state (See FIG. 1.) This result implies that the non-identical population can distinctly influence decoherence speed under dephasing dynamics which is attributed to the population-dependent coherence measure.

Dissipative dynamics.- To better understand the coherence of QSL, we further consider the dissipative dynamics. Suppose a two-level atom interacts with a leaky single-mode cavity [27, 85, 87]. The Hamiltonian of this system reads

$$H_{\text{tot}} = \frac{1}{2}\omega_0\sigma_z + \sum_j \omega_j b_j^\dagger b_j + \sum_j g_j \sigma_+ b_j + \text{h.c.}, \quad (23)$$

where various operators are defined analogous to those in Eq. (10). If the environment is a vacuum at the initial moment, one can derive the master equation of the reduced system as

$$\dot{\rho}_t = \frac{\gamma_t}{2} (2\sigma_- \rho_t \sigma_+ - \{\sigma_+ \sigma_-, \rho_t\}), \quad (24)$$

where ρ_t is the density matrix of the system of interest, and γ_t is the time-dependent decay rate. If the initial state of the system is given by Eq. (12), then one can solve Eq. (24) and get the density matrix ρ_t as

$$\rho_t = \begin{pmatrix} q_{11}(t) & q_{01}(t) \\ q_{01}^*(t) & 1 - q_{11}(t) \end{pmatrix} \quad (25)$$

with $q_{11}(t) = 1 - \rho_{11} e^{-\int_0^t dt' \gamma_{t'}}$ and $q_{01}(t) = \rho_{10} e^{-\int_0^t dt' \gamma_{t'}/2}$. Here we study τ_{CSL} dependent on the evolution time τ numerically. The figure is shown in FIG. 3 (Right), where the initial state and decay rate parameters are the same as the numerical example in the

dephasing model. Our bound is larger than the bound in Ref. [39], which indicates our bound has better tightness. Besides, according to the numerical result in FIG. 3 (Right), the initial state with identical entries ($\theta = \pi/2$) shows lower decoherence speed compared with the cases of $\theta = \pi/3$ and $\theta = \pi/4$. This result is exactly opposite to the results in the dephasing dynamics. The initial states with the same diagonal entries show the maximum decoherence speed for the dephasing case. However, in the JC model, the initial state with asymmetric diagonal entries exhibits a large decoherence speed. This phenomenon can be understood as follows. For the initial states with small non-diagonal entries, the main contribution to the evolution speed comes from the variation of the diagonal entries. The evolution trajectory derived from mere variation of the diagonal entries of the density matrix is closer to the geodesic, so even if the initial states with asymmetric diagonal elements do not decohere along the most direct path, they exhibit greater dynamical speed. We compare the bound presented by Ref. [39].

Attainability.- To gain further insight into the attainability of our coherence speed limit bound, we consider the geodesics ρ_t , $t \in [0, \tau]$ such that $\rho_t^* = \rho_0^*$ for $\forall t$, the geodesics has been explicitly given in Refs. [88, 89]. It is shown that the geodesics connecting ρ_0 and ρ_τ reads

$$\rho_t = \frac{[(1-p_t)\sqrt{\rho_0} + p_t\sqrt{\rho_\tau}]^2}{\text{Tr}[(1-p_t)\sqrt{\rho_0} + p_t\sqrt{\rho_\tau}]^2}, \quad (26)$$

the uniqueness of $\sqrt{\rho_t}$ indicates that

$$\sqrt{\rho_t} = \frac{(1-p_t)\sqrt{\rho_0} + p_t\sqrt{\rho_\tau}}{\sqrt{(1-p_t)^2 + p_t^2 + 2p_t(1-p_t)\text{Tr}\sqrt{\rho_0}\sqrt{\rho_\tau}}} \quad (27)$$

with monotonic real function p_t satisfying $p_0 = 0$ and $p_\tau = 1$. The space consisting of all the density matrices equipping the Wigner-Yanase metric is partly the Euclidean sphere [89], hence the geodesics Eq. (27) is a linear combination of $\sqrt{\rho_0}$ and $\sqrt{\rho_\tau}$, with the normalized numerator guaranteeing the length of $\sqrt{\rho_t}$ is unit, i.e., $\text{Tr}\rho_t = 1$, which is an immediately consequence of the sphere geometry [89]. For integrity, we provide an alternative method to showing the geodesics connecting ρ_0 and ρ_τ in Appendix B, apart from Refs. [88, 89]. The closest incoherent state to $\sqrt{\rho_t}$ is [81]

$$\rho_t^* = \sum_{i=1}^N \frac{\langle i | \sqrt{\rho_t} | i \rangle^2}{\sum_{j=1}^N \langle j | \sqrt{\rho_t} | j \rangle^2} | i \rangle \langle i | = \sum_{i=1}^N \frac{(\langle i | \sqrt{\rho_0} | i \rangle - p_t \langle i | (\sqrt{\rho_0} - \sqrt{\rho_\tau}) | i \rangle)^2}{\sum_{j=1}^N (\langle j | \sqrt{\rho_0} | j \rangle - p_t \langle j | (\sqrt{\rho_0} - \sqrt{\rho_\tau}) | j \rangle)^2} | i \rangle \langle i |. \quad (28)$$

From Eq. (6) and Eq. (8), one can immediately find that the saturated CSL needs $\rho_0^* = \rho_\tau^*$. Namely, ρ_t^* (Eq. (28)) shouldn't depend on time. Obviously, if

$$\langle i | \sqrt{\rho_t} | i \rangle = \langle j | \sqrt{\rho_t} | j \rangle \quad (29)$$

or

$$\langle i | \sqrt{\rho_0} | i \rangle = \langle i | \sqrt{\rho_\tau} | i \rangle \quad (30)$$

for $\forall t \in [0, \tau]$, $\forall i, j$, Eq. (28) will be time-independent.

Eq. (29) shows that the matrix $\sqrt{\rho_t}$ should have the same diagonal density entries, which indicates that ρ_t in 2 dimension should have identical diagonal entries, i.e., $\frac{1}{2}$, this characteristic can be only generated by the purely dephasing channel. However, this could differ for high-dimensional density matrices, which need further study due to their complexity. The density matrix ρ_t will have to own some particular form to guarantee the identical diagonal entries of $\sqrt{\rho_t}$. Similarly, Eq. (30) indicates that the diagonal entries of $\sqrt{\rho_t}$ shouldn't depend on time t . For a 2-dimensional density matrix, Eq. (30) means $\rho_0 = \rho_\tau$, which is a trivial case. Under the condition Eq. (29), dephasing dynamics is the only solution to saturate our speed limit bound in 2 dimension.

IV. CONCLUSION AND DISCUSSION

This paper establishes a quantum speed limit for coherence variation based on the skew information coherence measure. This QSL provides a lower bound on how long it takes for a physical system to generate or lose certain coherence. The results indicate that the classical Fisher information and the Wigner-Yanase skew information contribute two important fractions to the average evaluation speed. The non-vanishing Wigner-Yanase skew information corresponding to some unitary evolution often prevents the dynamics from evolving along the geodesics, which can be further verified in Appendix D, where we have also shown that the unitary evolution cannot be along the geodesics. Hence, the free Hamiltonian (unitary evolution) slow the evolution during the coherence variation in the case we raised. In this sense, the potential candidate could be the dynamics between degenerated energy levels or some particularly designed case, as shown in the above section. In addition, we also derive the saturation condition of our QSL bound. We find one condition is that the square root of quantum states during the evolution keep identical diagonal entries. In particular, in two-dimensional systems, this saturation condition needs the state to have the same populations during the evolution. That is, our QSL bound is attainable only in a two-level system with identical populations undergoing a purely dephasing channel with the constant-sign dephasing rate. Thus, one conclusion is that coherence-generating dynamics cannot evolve along the geodesics for a two-dimensional system, but decoherence can. Roughly speaking, coherence generation should be slower than decoherence. What's more, one can find that the coherence QSL bound depends on the populations, which is intuitively attributed to the fact that the skew information coherence measure depends on the populations and simultaneously induces a population-dependent metric, but essentially, the evolution trajec-

tory of density matrices depends on initial states as well as their populations. The dissipative dynamics can further understand this behavior. Unlike dephasing dynamics, we find that the states with the same diagonal entries exhibit less decoherence speed for the dissipative dynamics because the initial states with asymmetric diagonal entries own the evolution trajectory close to the geodesics. These two opposite results indicate the factors of decoherence for the different dynamics. Comparing our bound with that in Ref. [39], our bound exhibits relatively preferable compactness. Since quantum coherence is a fundamental feature of a quantum system, our coherence QSL bound reveals the lower bound of the transition time from quantum to classical features.

V. ACKNOWLEDGEMENTS

This work was supported by the National Natural Science Foundation of China under Grants Nos. 12175029, 12011530014.

APPENDIX A: THE PHYSICS OF WIGNER-YANASE METRIC FOR OPEN SYSTEM

In this appendix, we show the physical meaning of the W-Y metric. First, for arbitrarily given time-dependent density matrix ρ_t can be decomposed as [51]

$$\rho_t = U_t \Lambda_t U_t^\dagger = \left(U_t \sqrt{\Lambda_t} U_t^\dagger \right)^2, \quad (31)$$

where U_t is a time-dependent unitary matrix, and $\Lambda_t = \sum_i \lambda_i(t) |i\rangle\langle i|$ with $|i\rangle$ denoting the i -th eigenvector of ρ_0 . The uniqueness of $\sqrt{\rho_t}$ indicates that

$$\sqrt{\rho_t} = U_t \sqrt{\Lambda_t} U_t^\dagger = \sum_i \sqrt{\lambda_i(t)} U_t |i\rangle\langle i| U_t^\dagger, \quad (32)$$

and its derivative is expressed as

$$\frac{d}{dt} \sqrt{\rho_t} = \dot{U}_t U_t^\dagger \sqrt{\rho_t} + \sqrt{\rho_t} U_t \dot{U}_t^\dagger + \sum_i \left(\frac{d}{dt} \sqrt{\lambda_i(t)} \right) |i(t)\rangle\langle i(t)|, \quad (33)$$

where $|i(t)\rangle = U_t |i\rangle$ is the i -th eigenvector of ρ_t . By defining the effective Hamiltonian $H_t = i \dot{U}_t U_t^\dagger$, it's not difficult to find that H_t is hermitian, then one will immediately find that

$$\frac{d}{dt} \sqrt{\rho_t} = -i [H_t, \sqrt{\rho_t}] + \sum_i \left(\frac{d}{dt} \sqrt{\lambda_i(t)} \right) |i(t)\rangle\langle i(t)|, \quad (34)$$

then the W-Y metric is

$$\begin{aligned} \text{Tr} \left(\frac{d}{dt} \sqrt{\rho_t} \right)^2 &= \sum_j \left(\frac{d}{dt} \sqrt{\lambda_j(t)} \right)^2 - \text{Tr} [\sqrt{\rho_t}, H_t]^2 \\ &+ 2i \text{Tr} \left(\sum_j \left(\frac{d}{dt} \sqrt{\lambda_j(t)} \right) |j\rangle \langle j| [\sqrt{\rho_t}, H_t] \right), \end{aligned} \quad (35)$$

where the final term in the second line vanishes due to the commutative $\sqrt{\rho_t}$ and $\sum_j \frac{d}{dt} \sqrt{\lambda_j(t)} |j\rangle \langle j|$. Hence

$$\text{Tr} \left(\frac{d}{dt} \sqrt{\rho_t} \right)^2 = \frac{1}{4} \mathcal{I}_F + 2 \mathcal{I}_{W-Y}, \quad (36)$$

where $\mathcal{I}_F = 4 \sum_j \left(\frac{d}{dt} \sqrt{\lambda_j(t)} \right)^2$ and $\mathcal{I}_{W-Y} = -\frac{1}{2} \text{Tr} [\sqrt{\rho_t}, H_t]^2$ are the classical Fisher information and the Wigner-Yanase skew information, respectively. The classical Fisher information and the skew information of the effective Hamiltonian quantifies the sensitivity of the state ρ_t to a CPTP map due to classical and quantum effects, respectively [51, 84].

APPENDIX B: THE GEODESICS CONCERNING THE WIGNER-YANASE METRIC

We want to refer to Refs. ([88, 89]) to give the geodesic. Let's first consider a real vector space \mathbb{R}^N , \mathbf{r}_0 and \mathbf{r}_τ are arbitrarily given pair of normalized vectors, i.e., $|\mathbf{r}_{0,\tau}| = 1$, and $\mathbf{r}_0 \neq -\mathbf{r}_\tau$. Then

$$\mathbf{r}_t = \frac{p_t \mathbf{r}_0 + (1 - p_t) \mathbf{r}_\tau}{|p_t \mathbf{r}_0 + (1 - p_t) \mathbf{r}_\tau|} \quad (37)$$

is the normalized vector within the plane expanded by \mathbf{r}_0 and \mathbf{r}_τ , where p_t is the monotonic function satisfying $p_0 = 1$ and $p_\tau = 0$. Obviously, on a two-dimensional plane, the following triangle inequality is always saturated:

$$\arccos \langle \mathbf{r}_0, \mathbf{r}_\tau \rangle = \arccos \langle \mathbf{r}_0, \mathbf{r}_t \rangle + \arccos \langle \mathbf{r}_t, \mathbf{r}_\tau \rangle, \quad (38)$$

where

$$\begin{aligned} \langle \mathbf{r}_0, \mathbf{r}_t \rangle &= \frac{p_t + (1 - p_t) \langle \mathbf{r}_0, \mathbf{r}_\tau \rangle}{\sqrt{p_t^2 + (1 - p_t)^2 + 2p_t(1 - p_t) \langle \mathbf{r}_0, \mathbf{r}_\tau \rangle}} \equiv f_{p_t}(\langle \mathbf{r}_0, \mathbf{r}_\tau \rangle) \\ \langle \mathbf{r}_t, \mathbf{r}_\tau \rangle &= \frac{p_t \langle \mathbf{r}_0, \mathbf{r}_\tau \rangle + (1 - p_t)}{\sqrt{p_t^2 + (1 - p_t)^2 + 2p_t(1 - p_t) \langle \mathbf{r}_0, \mathbf{r}_\tau \rangle}} \equiv g_{p_t}(\langle \mathbf{r}_0, \mathbf{r}_\tau \rangle). \end{aligned} \quad (39)$$

One should notice that the above equations are satisfied for $\forall \langle \mathbf{r}_0, \mathbf{r}_\tau \rangle \in (-1, 1)$ and $p_t \in [0, 1]$. Hence

$$\arccos x = \arccos f_{p_t}(x) + \arccos g_{p_t}(x) \quad (40)$$

hold for any input $x \in (-1, 1)$ and $p_t \in [0, 1]$. Let $x = \text{Tr} \sqrt{\rho_0} \sqrt{\rho_\tau}$, it's not difficult to find that it equals to

$$\Theta(\rho_0, \rho_\tau) = \Theta(\rho_0, \rho_t) + \Theta(\rho_t, \rho_\tau) \quad (41)$$

for $\forall p_t \in [0, 1]$, it indicates that Eq. (27) is the geodesics connecting $\sqrt{\rho_0}$ and $\sqrt{\rho_\tau}$.

APPENDIX C: THE DERIVATION OF THE WIGNER-YANASE METRIC

To provide a clear theoretical framework, we'd like to present a derivation of the form of the Wigner-Yanase metric. First, considering an affinity function

$$A(\rho_t; s) = A(\rho_t, \rho_s) = \text{Tr} \sqrt{\rho_t} \sqrt{\rho_s} \quad (42)$$

with respect to one parameter $s \in [0, \tau]$ and ρ_t is a curve $t : 0 \rightarrow \tau$ in the state space. When s is close to t , one can expand A to the second order with respect to s as

$$A(\rho_t; s) = A(\rho_t, t) + \frac{\partial}{\partial s} A(\rho_t; s) \Big|_{s=t} dt + \frac{1}{2} \frac{\partial^2}{\partial s^2} A(\rho_t; s) \Big|_{s=t} dt^2 \quad (43)$$

with $dt = s - t$. It can be calculated that $A(\rho_t; t) = \text{Tr} \rho_t = 1$, $\frac{\partial}{\partial s} A(\rho_t; s) \Big|_{s=t} = \text{Tr} \sqrt{\rho_t} \frac{d}{dt} \sqrt{\rho_t} = 0$ and $\frac{\partial^2}{\partial s^2} A(\rho_t; s) \Big|_{s=t} = \text{Tr} \sqrt{\rho_t} \frac{d^2}{dt^2} \sqrt{\rho_t} = -\text{Tr} \left(\frac{d}{dt} \sqrt{\rho_t} \right)^2$, hence

$$A(\rho_t; s) = \text{Tr} \sqrt{\rho_t} \sqrt{\rho_s} = 1 - \frac{1}{2} \text{Tr} \left(\frac{d}{dt} \sqrt{\rho_t} \right)^2 \quad (44)$$

holds for s approaching t . Hence for any pair of neighboring states ρ_t and ρ_{t+dt} , the affinity is given as

$$\begin{aligned} A(\rho_t, \rho_{t+dt}) &= 1 - \frac{1}{2} \text{Tr} \left(\frac{d}{dt} \sqrt{\rho_t} \right)^2 \\ &= \cos \Theta(\rho_t, \rho_{t+dt}) = 1 - \frac{1}{2} \Theta^2(\rho_t, \rho_{t+dt}). \end{aligned} \quad (45)$$

Then, one can immediately observe that the Wigner-Yanase metric is

$$\Theta^2(\rho_t, \rho_{t+dt}) = \text{Tr} \left(\frac{d}{dt} \sqrt{\rho_t} \right)^2. \quad (46)$$

APPENDIX D: UNITARY EVOLUTION DEVIATES THE GEODESICS

Let's first assume that the unitary evolution in Eq. (27) can be expressed as $\sqrt{\rho_t} = U_t \sqrt{\rho_0} U_t^\dagger$. It can shown that this expression is invalid. For our assumption, it's not difficult to observe that $\text{Tr} \sqrt{\rho_t}$ is invariant for $\forall t \in [0, \tau]$. Then one can immediately get

$$\text{Tr} \sqrt{\rho_t} = \frac{1}{\sqrt{1 - 2p_t(1 - p_t)(1 - \text{Tr} \sqrt{\rho_0} \sqrt{\rho_\tau})}}. \quad (47)$$

It can be seen that, time-independence of the term $\text{Tr} \sqrt{\rho_t}$ requires $\text{Tr} \sqrt{\rho_0} \sqrt{\rho_\tau} = 1 \Leftrightarrow \rho_0 = \rho_\tau$. Hence $\sqrt{\rho_t} = U_t \sqrt{\rho_0} U_t^\dagger$ is valid only for $U_t = \mathbb{I}$, which is a trivial case.

-
- [1] L. Mandelstam and I. Tamm, The uncertainty relation between energy and time in nonrelativistic quantum mechanics, *J. Phys.(USSR)* **9**, 249 (1945).
- [2] N. Margolus and L. B. Levitin, The maximum speed of dynamical evolution, *Physica D: Nonlinear Phenomena* **120**, 188 (1998), proceedings of the Fourth Workshop on Physics and Consumption.
- [3] L. B. Levitin and T. Toffoli, Fundamental limit on the rate of quantum dynamics: The unified bound is tight, *Phys. Rev. Lett.* **103**, 160502 (2009).
- [4] M. R. Frey, Quantum speed limits—primer, perspectives, and potential future directions, *Quantum Information Processing* **15**, 3919 (2016).
- [5] S. Deffner and S. Campbell, Quantum speed limits: from heisenberg’s uncertainty principle to optimal quantum control, *Journal of Physics A: Mathematical and Theoretical* **50**, 453001 (2017).
- [6] V. Giovannetti, S. Lloyd, and L. Maccone, Quantum limits to dynamical evolution, *Phys. Rev. A* **67**, 052109 (2003).
- [7] Y.-J. Zhang, W. Han, Y.-J. Xia, J.-P. Cao, and H. Fan, Quantum speed limit for arbitrary initial states, *Scientific reports* **4**, 4890 (2014).
- [8] J. Anandan and Y. Aharonov, Geometry of quantum evolution, *Phys. Rev. Lett.* **65**, 1697 (1990).
- [9] F. Campaioli, F. A. Pollock, F. C. Binder, and K. Modi, Tightening quantum speed limits for almost all states, *Phys. Rev. Lett.* **120**, 060409 (2018).
- [10] P. J. Jones and P. Kok, Geometric derivation of the quantum speed limit, *Phys. Rev. A* **82**, 022107 (2010).
- [11] M. Zwierz, Comment on “geometric derivation of the quantum speed limit”, *Phys. Rev. A* **86**, 016101 (2012).
- [12] S. Sun and Y. Zheng, Distinct bound of the quantum speed limit via the gauge invariant distance, *Phys. Rev. Lett.* **123**, 180403 (2019).
- [13] G. Ness, A. Alberti, and Y. Sagi, Quantum speed limit for states with a bounded energy spectrum, *Phys. Rev. Lett.* **129**, 140403 (2022).
- [14] D. A. Lidar, P. Zanardi, and K. Khodjasteh, Distance bounds on quantum dynamics, *Phys. Rev. A* **78**, 012308 (2008).
- [15] A. del Campo, I. L. Egusquiza, M. B. Plenio, and S. F. Huelga, Quantum speed limits in open system dynamics, *Phys. Rev. Lett.* **110**, 050403 (2013).
- [16] E. O’Connor, G. Guarnieri, and S. Campbell, Action quantum speed limits, *Phys. Rev. A* **103**, 022210 (2021).
- [17] K. Funo, N. Shiraishi, and K. Saito, Speed limit for open quantum systems, *New Journal of Physics* **21**, 013006 (2019).
- [18] N. Mirkin, F. Toscano, and D. A. Wisniacki, Quantum-speed-limit bounds in an open quantum evolution, *Phys. Rev. A* **94**, 052125 (2016).
- [19] A. Ektesabi, N. Behzadi, and E. Faizi, Improved bound for quantum-speed-limit time in open quantum systems by introducing an alternative fidelity, *Phys. Rev. A* **95**, 022115 (2017).
- [20] F. Campaioli, F. A. Pollock, and K. Modi, Tight, robust, and feasible quantum speed limits for open dynamics, *Quantum* **3**, 168 (2019).
- [21] Z.-y. Mai and C.-s. Yu, Tight and attainable quantum speed limit for open systems, *Phys. Rev. A* **108**, 052207 (2023).
- [22] N. Il’in and O. Lychkovskiy, Quantum speed limit for thermal states, *Phys. Rev. A* **103**, 062204 (2021).
- [23] Y. Shao, B. Liu, M. Zhang, H. Yuan, and J. Liu, Operational definition of a quantum speed limit, *Phys. Rev. Res.* **2**, 023299 (2020).
- [24] S.-x. Wu and C.-s. Yu, Quantum speed limit for a mixed initial state, *Phys. Rev. A* **98**, 042132 (2018).
- [25] D. P. Pires, M. Cianciaruso, L. C. Céleri, G. Adesso, and D. O. Soares-Pinto, Generalized geometric quantum speed limits, *Phys. Rev. X* **6**, 021031 (2016).
- [26] M. M. Taddei, B. M. Escher, L. Davidovich, and R. L. de Matos Filho, Quantum speed limit for physical processes, *Phys. Rev. Lett.* **110**, 050402 (2013).
- [27] S. Deffner and E. Lutz, Quantum speed limit for non-markovian dynamics, *Phys. Rev. Lett.* **111**, 010402 (2013).
- [28] X. Cai and Y. Zheng, Quantum dynamical speedup in a nonequilibrium environment, *Phys. Rev. A* **95**, 052104 (2017).
- [29] Y.-J. Zhang, W. Han, Y.-J. Xia, J.-P. Cao, and H. Fan, Classical-driving-assisted quantum speed-up, *Phys. Rev. A* **91**, 032112 (2015).
- [30] H.-B. Liu, W. L. Yang, J.-H. An, and Z.-Y. Xu, Mechanism for quantum speedup in open quantum systems, *Phys. Rev. A* **93**, 020105 (2016).
- [31] Z. Sun, J. Liu, J. Ma, and X. Wang, Quantum speed limits in open systems: Non-markovian dynamics without rotating-wave approximation, *Scientific reports* **5**, 8444 (2015).
- [32] M. Cianciaruso, S. Maniscalco, and G. Adesso, Role of non-markovianity and backflow of information in the speed of quantum evolution, *Phys. Rev. A* **96**, 012105 (2017).
- [33] I. Marvian and D. A. Lidar, Quantum speed limits for leakage and decoherence, *Phys. Rev. Lett.* **115**, 210402 (2015).
- [34] K. Lan, S. Xie, and X. Cai, Geometric quantum speed limits for markovian dynamics in open quantum systems, *New Journal of Physics* **24**, 055003 (2022).
- [35] X. Hu, S. Sun, and Y. Zheng, Witnessing localization of a quantum state via quantum speed limits in a driven avoided-level crossing system, *The Journal of Chemical Physics* **156**, 134113 (2022), https://pubs.aip.org/aip/jcp/article-pdf/doi/10.1063/5.0078207/16539484/134113_1_online.pdf.
- [36] L. Zheng and Y. Peng, Quantum speed limits of quantum system in colored environments, *Results in Physics* **57**, 107315 (2024).
- [37] I. Marvian, R. W. Spekkens, and P. Zanardi, Quantum speed limits, coherence, and asymmetry, *Phys. Rev. A* **93**, 052331 (2016).
- [38] D. Mondal, C. Datta, and S. Sazim, Quantum coherence sets the quantum speed limit for mixed states, *Physics Letters A* **380**, 689 (2016).
- [39] B. Mohan, S. Das, and A. K. Pati, Quantum speed limits for information and coherence, *New Journal of Physics* **24**, 065003 (2022).
- [40] B. Shanahan, A. Chenu, N. Margolus, and A. del Campo, Quantum speed limits across the quantum-to-classical transition, *Phys. Rev. Lett.* **120**, 070401 (2018).

- [41] M. Okuyama and M. Ohzeki, Quantum speed limit is not quantum, *Phys. Rev. Lett.* **120**, 070402 (2018).
- [42] T. Caneva, M. Murphy, T. Calarco, R. Fazio, S. Montangero, V. Giovannetti, and G. E. Santoro, Optimal control at the quantum speed limit, *Phys. Rev. Lett.* **103**, 240501 (2009).
- [43] V. Giovannetti, S. Lloyd, and L. Maccone, Advances in quantum metrology, *Nature photonics* **5**, 222 (2011).
- [44] V. Giovannetti, S. Lloyd, and L. Maccone, Quantum metrology, *Phys. Rev. Lett.* **96**, 010401 (2006).
- [45] A. W. Chin, S. F. Huelga, and M. B. Plenio, Quantum metrology in non-markovian environments, *Phys. Rev. Lett.* **109**, 233601 (2012).
- [46] B. Mohan and A. K. Pati, Quantum speed limits for observables, *Phys. Rev. A* **106**, 042436 (2022).
- [47] B. Mohan and A. K. Pati, Reverse quantum speed limit: How slowly a quantum battery can discharge, *Phys. Rev. A* **104**, 042209 (2021).
- [48] S. Campbell, M. G. Genoni, and S. Deffner, Precision thermometry and the quantum speed limit, *Quantum Science and Technology* **3**, 025002 (2018).
- [49] J. Liu and H. Nie, Initial-state-dependent quantum speed limit for dissipative state preparation: Framework and optimization, *Phys. Rev. A* **107**, 052608 (2023).
- [50] S. Sun, Y. Peng, X. Hu, and Y. Zheng, Quantum speed limit quantified by the changing rate of phase, *Phys. Rev. Lett.* **127**, 100404 (2021).
- [51] L. P. García-Pintos, S. B. Nicholson, J. R. Green, A. del Campo, and A. V. Gorshkov, Unifying quantum and classical speed limits on observables, *Phys. Rev. X* **12**, 011038 (2022).
- [52] K. Kobayashi and N. Yamamoto, Quantum speed limit for robust state characterization and engineering, *Phys. Rev. A* **102**, 042606 (2020).
- [53] X.-M. Zhang, Z.-W. Cui, X. Wang, and M.-H. Yung, Automatic spin-chain learning to explore the quantum speed limit, *Phys. Rev. A* **97**, 052333 (2018).
- [54] F. Campaioli, C.-s. Yu, F. A. Pollock, and K. Modi, Resource speed limits: maximal rate of resource variation, *New Journal of Physics* **24**, 065001 (2022).
- [55] X. Shi, Coherence quantifier based on the quantum optimal transport cost, *Phys. Rev. A* **109**, 052443 (2024).
- [56] B. Mohan, S. Das, and A. K. Pati, Quantum speed limits for information and coherence, *New Journal of Physics* **24**, 065003 (2022).
- [57] F. Sakuldee and L. Rudnicki, Bounds on the breaking time for entanglement-breaking channels, *Phys. Rev. A* **107**, 022430 (2023).
- [58] D. Shrimali, S. Bhowmick, V. Pandey, and A. K. Pati, Capacity of entanglement for a nonlocal hamiltonian, *Phys. Rev. A* **106**, 042419 (2022).
- [59] V. Pandey, S. Bhowmick, B. Mohan, Sohail, and U. Sen, Fundamental speed limits on entanglement dynamics of bipartite quantum systems (2023), [arXiv:2303.07415 \[quant-ph\]](https://arxiv.org/abs/2303.07415).
- [60] V. Pandey, D. Shrimali, B. Mohan, S. Das, and A. K. Pati, Speed limits on correlations in bipartite quantum systems, *Phys. Rev. A* **107**, 052419 (2023).
- [61] G. S. Engel, T. R. Calhoun, E. L. Read, T.-K. Ahn, T. Mančal, Y.-C. Cheng, R. E. Blankenship, and G. R. Fleming, Evidence for wavelike energy transfer through quantum coherence in photosynthetic systems, *Nature* **446**, 782 (2007).
- [62] M. B. Plenio and S. F. Huelga, Dephasing-assisted transport: quantum networks and biomolecules, *New Journal of Physics* **10**, 113019 (2008).
- [63] E. Collini, C. Y. Wong, K. E. Wilk, P. M. Curmi, P. Brumer, and G. D. Scholes, Coherently wired light-harvesting in photosynthetic marine algae at ambient temperature, *Nature* **463**, 644 (2010).
- [64] S. Lloyd, Quantum coherence in biological systems, in *Journal of Physics-Conference Series*, Vol. 302 (2011) p. 012037.
- [65] C.-M. Li, N. Lambert, Y.-N. Chen, G.-Y. Chen, and F. Nori, Witnessing quantum coherence: from solid-state to biological systems, *Scientific reports* **2**, 885 (2012).
- [66] S. F. Huelga and M. B. Plenio, Vibrations, quanta and biology, *Contemporary Physics* **54**, 181 (2013).
- [67] L. Rybak, S. Amaran, L. Levin, M. Tomza, R. Moszynski, R. Kosloff, C. P. Koch, and Z. Amitay, Generating molecular rovibrational coherence by two-photon femtosecond photoassociation of thermally hot atoms, *Phys. Rev. Lett.* **107**, 273001 (2011).
- [68] J. Åberg, Catalytic coherence, *Phys. Rev. Lett.* **113**, 150402 (2014).
- [69] V. Narasimhachar and G. Gour, Low-temperature thermodynamics with quantum coherence, *Nature communications* **6**, 7689 (2015).
- [70] P. Ćwikliński, M. Studziński, M. Horodecki, and J. Oppenheim, Towards fully quantum second laws of thermodynamics: limitations on the evolution of quantum coherences, [arXiv preprint arXiv:1405.5029](https://arxiv.org/abs/1405.5029) (2014).
- [71] M. Lostaglio, D. Jennings, and T. Rudolph, Description of quantum coherence in thermodynamic processes requires constraints beyond free energy, *Nature communications* **6**, 6383 (2015).
- [72] M. Lostaglio, K. Korzekwa, D. Jennings, and T. Rudolph, Quantum coherence, time-translation symmetry, and thermodynamics, *Phys. Rev. X* **5**, 021001 (2015).
- [73] P. Reberstrost, M. Mohseni, and A. Aspuru-Guzik, Role of quantum coherence and environmental fluctuations in chromophoric energy transport, *The Journal of Physical Chemistry B* **113**, 9942 (2009).
- [74] B. Witt and F. Mintert, Stationary quantum coherence and transport in disordered networks, *New Journal of Physics* **15**, 093020 (2013).
- [75] A. Streltsov, U. Singh, H. S. Dhar, M. N. Bera, and G. Adesso, Measuring quantum coherence with entanglement, *Phys. Rev. Lett.* **115**, 020403 (2015).
- [76] O. Karlström, H. Linke, G. Karlström, and A. Wacker, Increasing thermoelectric performance using coherent transport, *Phys. Rev. B* **84**, 113415 (2011).
- [77] T. Baumgratz, M. Cramer, and M. B. Plenio, Quantifying coherence, *Phys. Rev. Lett.* **113**, 140401 (2014).
- [78] C.-s. Yu and H.-s. Song, Bipartite concurrence and localized coherence, *Phys. Rev. A* **80**, 022324 (2009).
- [79] J. Ma, B. Yadin, D. Girolami, V. Vedral, and M. Gu, Converting coherence to quantum correlations, *Phys. Rev. Lett.* **116**, 160407 (2016).
- [80] C.-s. Yu, S.-r. Yang, and B.-q. Guo, Total quantum coherence and its applications, *Quantum Information Processing* **15**, 3773 (2016).
- [81] C.-s. Yu, Quantum coherence via skew information and its polygamy, *Phys. Rev. A* **95**, 042337 (2017).

- [82] Y.-C. Liang, Y.-H. Yeh, P. E. M. F. Mendonça, R. Y. Teh, M. D. Reid, and P. D. Drummond, Quantum fidelity measures for mixed states, [Reports on Progress in Physics](#) **82**, 076001 (2019).
- [83] S. Luo and Q. Zhang, Informational distance on quantum-state space, [Phys. Rev. A](#) **69**, 032106 (2004).
- [84] D. Girolami, How difficult is it to prepare a quantum state?, [Phys. Rev. Lett.](#) **122**, 010505 (2019).
- [85] H.-P. Breuer and F. Petruccione, *The theory of open quantum systems* (Oxford University Press on Demand, 2002).
- [86] A. Das, A. Bera, S. Chakraborty, and D. Chruściński, Thermodynamics and the quantum speed limit in the non-markovian regime, [Phys. Rev. A](#) **104**, 042202 (2021).
- [87] B. M. Garraway, Nonperturbative decay of an atomic system in a cavity, [Phys. Rev. A](#) **55**, 2290 (1997).
- [88] A. Jenčová, Geodesic distances on density matrices, [Journal of Mathematical Physics](#) **45**, 1787 (2004).
- [89] P. Gibilisco and T. Isola, Wigner–yanase information on quantum state space: the geometric approach, [Journal of Mathematical Physics](#) **44**, 3752 (2003).